

Outline of the High Resolution Global Model at the Japan Meteorological Agency

Masayuki Nakagawa

Numerical Prediction Division, Japan Meteorological Agency

Abstract

The Japan Meteorological Agency (JMA) upgraded the resolution of the Global Spectral Model (GSM) from TL319L40 to TL959L60 on 21 November 2007, when the Typhoon Model retired from operational use. Since then, tropical cyclone (TC) track and intensity forecasts have been supported by GSM only. GSM provides numerical weather prediction (NWP) products four times a day for all TCs existing globally. This paper gives an outline of the high resolution GSM and shows its performance in TC track and intensity forecasts.

1. Introduction

The Japan Meteorological Agency (JMA) provides a variety of numerical weather prediction (NWP) products that play a vital role in both national and international weather services. Among these, tropical cyclone (TC) track and intensity forecasts are the most important for disaster prevention and preparedness activities.

On 21 November 2007, the spatial resolution of the Global Spectral Model (GSM) was greatly enhanced from the previous TL319L40 (approximately 60 km in the horizontal and 40 layers up to 0.4 hPa in the vertical) to TL959L60 (approximately 20 km in the horizontal and 60 layers up to 0.1 hPa in the vertical) (Iwamura and Kitagawa 2008). Until that time, JMA had operated not only GSM (TL319L40) but also the 24-km resolution Typhoon Model (TYM), covering a TC and its surrounding areas to provide TC track and intensity forecasts. TYM had been run for two TCs at most for each initial time. Since the time of the increase of the resolution of GSM, when TYM retired from operational use, TC forecasts have been supported only by GSM covering the entire globe. GSM provides high resolution NWP products four times a day for all TCs worldwide.

In February 2008, JMA began the operation of a TC ensemble prediction system (the Typhoon Ensemble Prediction System, or TEPS) to improve both deterministic and probabilistic forecasts of TC movements after a period of preliminary operation from May 2007. For details of TEPS, see Yamaguchi and Komori (2009).

This paper describes the high resolution global NWP system. Section 2 introduces the major features and specifications of GSM. Section 3 gives examples and statistical scores of typhoon track

and intensity forecasts. A summary of the results and conclusions are presented in section 4.

2. Outline of the global NWP system

The specifications of the previous GSM, TYM, current GSM and TEPS are summarized in Table 1. The major changes made to GSM in November 2007 are as follows:

- an increase in the resolution from TL319L40 to TL959L60 with the topmost level raised from 0.4 hPa to 0.1 hPa,
- an increase in the resolution of the inner model of the four-dimensional variational (4D-Var) data assimilation system from T106L40 to T159L60,
- use of data from new high resolution analysis of sea surface temperature and sea ice concentration as ocean surface boundary conditions,
- use of surface snow depth data from the domestic dense observational network in global snow depth analysis,
- upgrade of the numerical integration scheme from a three-time-level leap-frog scheme to a two-time-level scheme,
- introduction of a new convective triggering scheme proposed by Xie and Zhang (2000) into the deep convection parameterization, and
- introduction of a new two-dimensional aerosol climatology derived from satellite observations for the radiation calculation.

Table 1 Framework of previous and current NWP models for TC forecasts at JMA

	Global Model (GSM, previous)	Typhoon Model (TYM, terminated)	Global Model (GSM, current)	Typhoon Ensemble Prediction System (TEPS)
Forecast domain	Global	TC and its surrounding areas	Global	
Grid size / Number of grids	0.5625 deg. / 640 x 320 (TL319)	24 km / 271 x 271	0.1875 deg. / 1920 (equator) – 6 deg. / 60 (closest to pole) x 960 (TL959)	0.5625 deg. / 640 x 320 (TL319)
Vertical levels/Top	40 / 0.4 hPa	25 / 17.5 hPa	60 / 0.1 hPa	
Forecast range (initial time)	90 hours (00UTC), 216 hours (12 UTC), 36 hours (06, 18 UTC)	84 hours (00, 06, 12, 18 UTC) Maximum 2 runs for each initial time	84 hours (00, 06, 18 UTC), 216 hours (12 UTC)	132 hours (00, 06, 12, 18 UTC) 11 members
Analysis	4D-Var	Global analysis	4D-Var	Global analysis with SV ensemble perturbations

For the global analysis, 4D-Var data assimilation method is employed. The control variables are relative vorticity, unbalanced divergence, unbalanced temperature, unbalanced surface pressure and the natural logarithm of specific humidity. In order to improve computational efficiency, an incremental method is adopted in which the analysis increment is first evaluated at a lower horizontal resolution (T159) before being interpolated and added to the first-guess field at the original resolution (TL959). The specifications of the atmospheric analysis schemes are listed in Table 2.

Global analyses are performed at 00, 06, 12 and 18 UTC every day. An early analysis with a short cut-off time is performed to prepare the initial conditions for operational forecast, and a cycle analysis with a long cut-off time is performed to pursue better quality of the global data assimilation system.

For TCs in the western North Pacific, typhoon bogus data are generated and assimilated for each TC to represent the structure accurately in the initial field for the forecast models. These consist of data relating to the artificial sea-surface pressure, temperature and wind data encircling each TC. The structure is axi-asymmetric. At first, a symmetric bogus profile is automatically generated based on the central pressure and 30-kt wind speed radius of the TC analyzed by forecasters. An axi-asymmetric bogus profile is then generated by retrieving asymmetric components from the first-guess field. The symmetric and axi-asymmetric profiles are combined to form the final bogus profile, which is then converted into pseudo-observation data for use in the global analysis.

GSM employs hydrostatic primitive equations with a shallow atmosphere assumption to express the resolvable motions and states of the atmosphere. The prognostic variables are wind (zonal and meridional), temperature, specific humidity, surface pressure and cloud water content. In

Table 2 Specifications of global objective analysis

Cut-off time	2 hr 20 min for early run analyses at 00, 06, 12 and 18 UTC, 11 hr 35 min for cycle run analyses at 00 and 12 UTC, 5 hr 35 min for cycle run analyses at 06 and 18 UTC
First guess	6-hour forecast by GSM
Grid form, resolution and number of grids	Reduced Gaussian grid, 0.1875-6 deg., 1920-60 x 960 for outer model Standard Gaussian grid, 0.75 deg., 480 x 240 for inner model
Levels	60 forecast model levels up to 0.1 hPa + surface
Analysis variables	Wind, surface pressure, temperature and specific humidity
Methodology	4D-Var scheme on model levels
Data used	SYNOP, SHIP, BUOY, TEMP, PILOT, Wind Profiler, AIREP, radiances from NOAA/ATOVS, MetOp/ATOVS, Aqua/AMSU-A, clear-sky radiances and atmospheric motion vectors (AMVs) from MTSAT-1R, GOES, METEOSAT, MODIS polar AMVs, SeaWinds, Microwave imager radiometer radiances (AMSR-E, TMI, SSM/I) and Australian PAOB; Typhoon bogussing applied for analysis
Initialization	Non-linear normal mode initialization for inner model

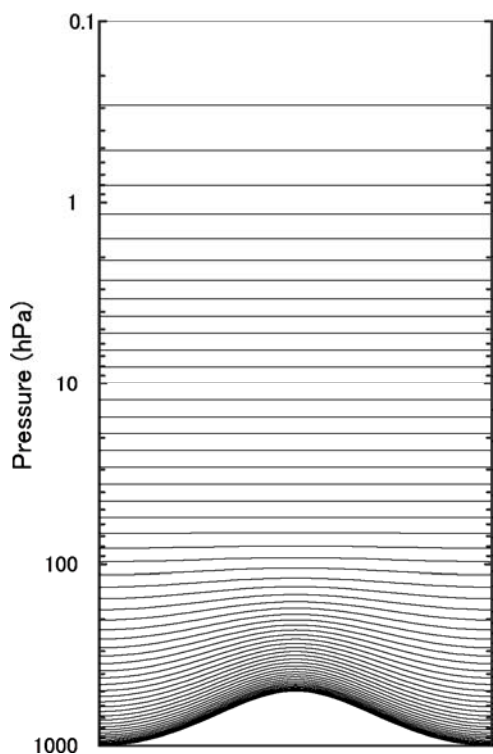


Figure 1 Distribution of vertical layers of GSM

(Yoshimura and Matsumura 2003) is adopted and fourth-order linear horizontal diffusion is applied. GSM also includes sophisticated parameterization schemes for physical processes such as gravity wave drag, planetary boundary layer, land surface, radiation, cumulus convection and cloud. JMA runs GSM four times a day (84-hour forecasts from 00, 06 and 18 UTC and 216-hour forecasts from 12 UTC). The specifications of GSM are listed in Table 3.

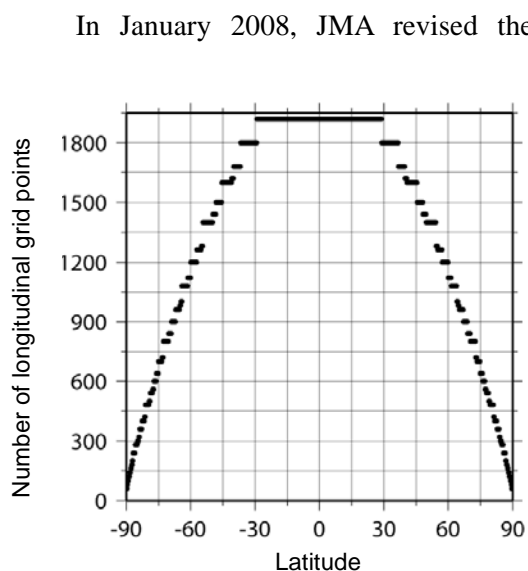


Figure 2 Number of longitudinal grid points against latitude in reduced Gaussian grid GSM (TL959)

the horizontal, the prognostic variables are spectrally discretized with a triangular truncation wave of 959 (TL959). The corresponding transform grids are spaced by about 0.1875 degrees representing about 20 km. Such high resolution enables detailed representation of land/sea mask and topography, which could improve forecasts of synoptic and sub-synoptic weather. In the vertical, a sigma-p hybrid coordinate is introduced. GSM has 60 layers up to 0.1 hPa as shown in Figure 1. The vertical resolution is higher in the lower atmosphere for better simulation of the planetary boundary layer processes. The raised topmost level helps to assimilate satellite observations more effectively.

The time integration is based on a two-time-level, semi-implicit semi-Lagrangian scheme. A vertically conservative semi-Lagrangian scheme (Yoshimura and Matsumura 2003) is adopted and fourth-order linear horizontal diffusion is applied. GSM also includes sophisticated parameterization schemes for physical processes such as gravity wave drag, planetary boundary layer, land surface, radiation, cumulus convection and cloud. JMA runs GSM four times a day (84-hour forecasts from 00, 06 and 18 UTC and 216-hour forecasts from 12 UTC). The specifications of GSM are listed in Table 3.

In January 2008, JMA revised the calculation procedure for the convective triggering mechanism in GSM to accurately consider the effect of wind crossing isobars at the surface, which had not been calculated correctly in the previous version (Nakagawa 2008). Excessive limitation of cumulus upward mass flux from a redundant vertical CFL condition was also removed.

In August 2008, a reduced Gaussian grid was implemented in GSM as a new dynamical core (Miyamoto 2006). On the standard Gaussian grid, the longitudinal interval between neighboring grid points decreases as the latitude increases. Hence, it is redundant to use an equal number of grid points for all given latitudes in a global model. The introduction of the reduced Gaussian grid removes

Table 3 Specifications of GSM

Basic equation	Primitive equations
Independent variables	Latitude, longitude and sigma-pressure hybrid coordinates and time
Dependent variables	Winds (zonal, meridional), temperature, specific humidity, surface pressure and cloud water content
Numerical technique	Spectral (spherical harmonics basis functions) in the horizontal Finite differences in the vertical Two-time-level, semi-Lagrangian, semi-implicit time integration scheme Hydrostatic approximation
Integration domain	Global in the horizontal Surface to 0.1 hPa in the vertical
Horizontal resolution	Spectral triangular 959 (TL959) roughly equivalent to 0.1875 x 0.1875 degrees lat-lon Reduced Gaussian grid, 1920 (equator) – 60 (pole) x 960
Vertical resolution	60 unevenly spaced sigma-p hybrid levels
Time step	10 minutes
Forecast time	84 hours from 00, 06 and 18 UTC, 216 hours from 12 UTC
Orography	GTOPO30 data set spectrally truncated and smoothed
Horizontal diffusion	Linear, fourth-order
Vertical diffusion	Stability (Richardson number) dependent, local formulation
Gravity wave drag	Longwave scheme (wavelengths > 100 km) mainly for stratosphere Shortwave scheme (wavelengths approx. 10 km) only for troposphere
Planetary boundary layer	Mellor and Yamada level-2 turbulence closure scheme Similarity theory in bulk formulae for surface layer
Treatment of sea surface	Climatological sea surface temperature with daily analyzed anomaly Climatological sea ice concentration with daily analyzed anomaly
Land surface	Simple Biosphere (SiB) model
Radiation	Two-stream with delta-Eddington approximation for shortwave Table look-up and k-distribution methods for longwave
Convection	Prognostic Arakawa-Schubert cumulus parameterization
Cloud	Prognostic cloud water, cloud cover diagnosed from moisture and cloud water

this redundancy by cutting grid points as shown in Figure 2, thus saving on computational resources. JMA is planning to introduce the reduced Gaussian grid to TEPS in the near future.

NWP products such as facsimile charts and Grid Point Value (GPV) data are disseminated through the JMA radio facsimile broadcast (JMH), the Global Telecommunication System (GTS), the RSMC Tokyo Data Serving System (RSMC DSS) and the World Meteorological Organization (WMO) Distributed Data Bases (DDBs) project server. Details of the NWP products disseminated are presented in the appendix.

3. Forecast of TC

3.1 Experimental design

In order to evaluate the forecast skill of the NWP system, forecast/assimilation experiments for TL959L60 GSM (August 2008 version with reduced Gaussian grid) and TL319L40 GSM (previous operational model) were conducted for August 2006 and January 2007. Starting from cycle analyses, 84-hour forecasts and 216-hour forecasts were performed with daily initiation at 00 UTC and 12 UTC, respectively. The forecasts of TCs in the responsibility area of the RSMC Tokyo - Typhoon Center (0° - 60° N, 100° - 180° E) were verified against the best track analyzed by the Center. The verified elements were the 84-hour forecasts of the center position, central pressure and maximum sustained winds. The results were compared to those of the operational TYM. In the statistical verification, samples in which all models were able to keep track of TCs were selected. It should be noted that the operational TYM started from initial fields based on early analysis of the operational TL319L40 GSM and used lateral boundary conditions interpolated from operational TL319L40 GSM forecasts starting from early analysis. As a result, the numbers of observation data used to make the TYM initial fields and lateral boundary conditions were less than those used to make the initial fields in the forecast/assimilation experiments for GSM, which may negatively affect the forecast skill of TYM.

3.2 Case study

Figure 3 shows the forecast track, central pressure and maximum sustained wind speed of Typhoon WUKONG (T0610) predicted by TL959L60 GSM, TL319L40 GSM and TYM along with the best track. The initial time of the forecasts is 12 UTC 16 August 2006. Moving to the northwest, WUKONG made landfall on Kyushu Island late on 17 August. After turning to the north, it weakened into a TD at 12UTC 19 August. TL959L60 GSM predicted the center position the best, while TL319L40 GSM and TYM showed westward and eastward error, respectively. As for the intensity of the typhoon, TL959L60 GSM could not sufficiently predict its weakening, which may be due to the poor representation of the effect of landfall. TL319L40 GSM predicted a weaker typhoon compared to the other models because of its low horizontal resolution. It was also unable to predict the weakening of the typhoon, due at least in part to it not making landfall on Kyushu Island. The typhoon predicted by TYM showed intensification in the early forecast hours. The tendency to predict larger development compared to TL959L60 GSM is a common feature in TYM forecast.

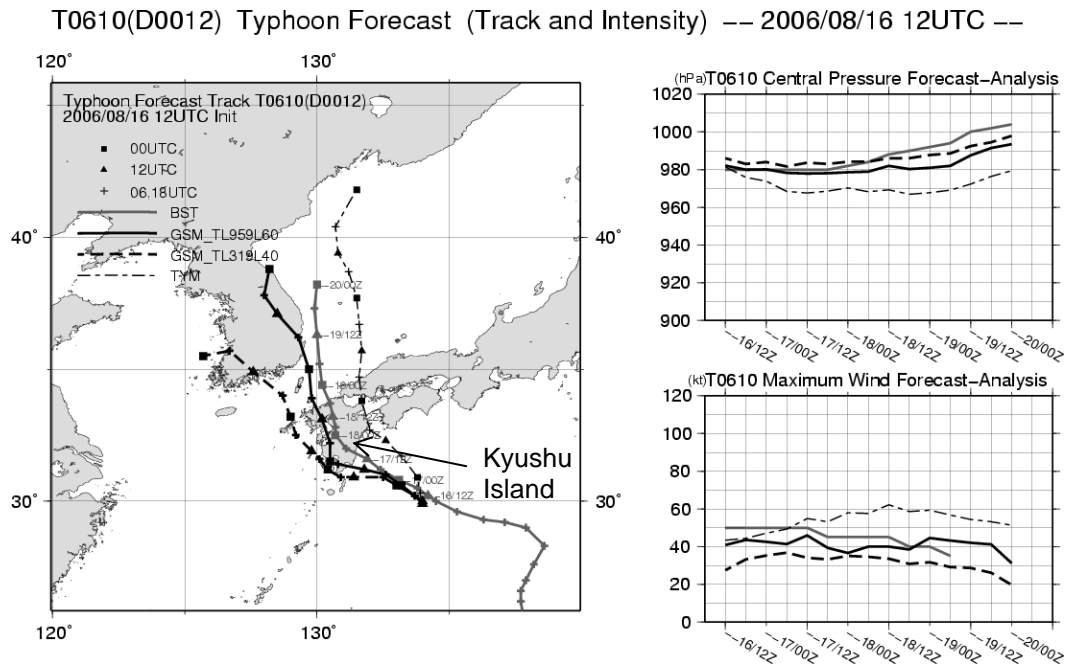


Figure 3 Predicted track (left), central pressure (top right) and maximum wind speed (bottom right) of T0610 (WUKONG). The initial time of the forecasts is 12 UTC 16 August 2006. The solid black line, broken black line, thin black dot-dash line and solid gray line indicate forecast by TL959L60 GSM, that by TL319L40 GSM, that by TYM and the analyzed best track, respectively.

The six-hour accumulated precipitations valid at 12 UTC 18 August 2006 in the forecasts by the three models and those analyzed are shown in Figure 4. The initial time of the forecasts is 12 UTC 17 August 2006, when Typhoon WUKONG was moving northward over Kyushu Island. All three models predicted the center position of the typhoon well in this case. Owing to its low horizontal resolution, TL319L40 GSM could not predict the detailed distribution of precipitation and strong rainfall over land caused by orographic effects. Although TYM represented orographic precipitation more strongly, its prediction of precipitation was too strong near the typhoon center and too weak away from the center. TL959L60 GSM simulated the distribution and intensity of precipitation better than other models, including orographic precipitation and heavy rainfall near the center of the

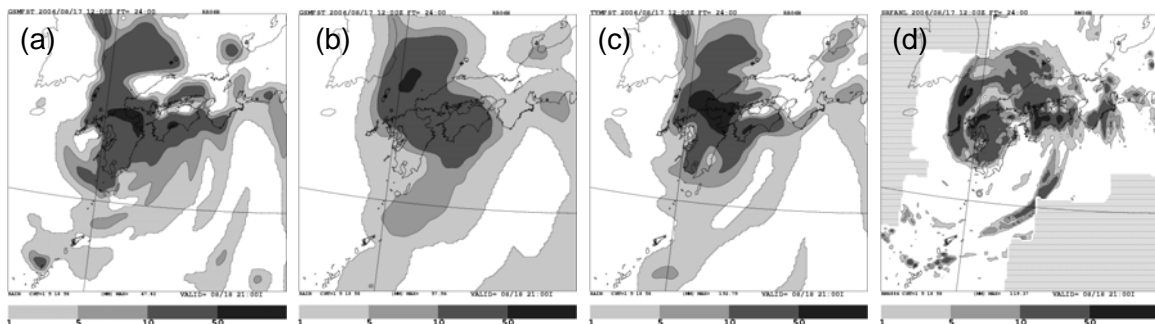


Figure 4 Six-hour accumulated precipitation valid at 12 UTC 18 August 2006. The initial time of the forecasts is 12 UTC 17 August 2006. (a): TL959L60 GSM forecast, (b): TL319L40 GSM forecast, (c): TYM forecast, (d): Radar-rain gauge analysis. The gray horizontal lines in (d) indicate an absence of analysis.

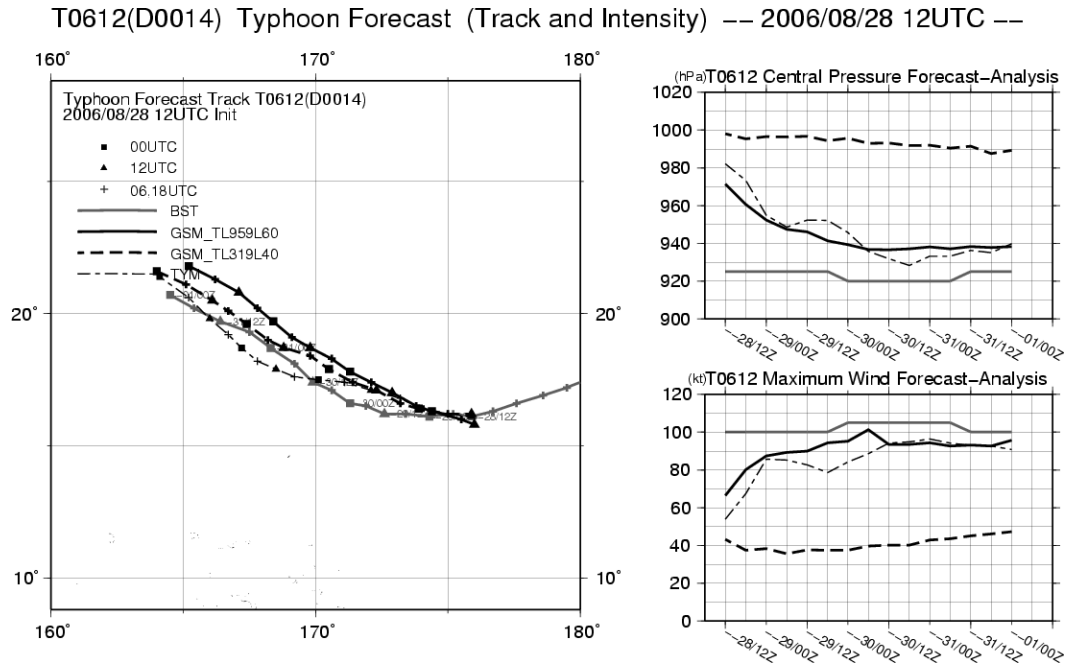


Figure 5 As Figure 3, but for T0612 (IOKE). The initial time of the forecasts is 12 UTC 28 August 2006.

typhoon.

Figure 5 shows the forecast track, central pressure and maximum sustained wind speed of Typhoon IOKE (T0612) predicted by the three models along with the best track. The initial time of the forecasts is 12 UTC 28 August 2006. IOKE turned to the west around the initial time and attained peak intensity with maximum sustained winds of 105 kt and a central pressure of 920 hPa over the sea southeast of Wake Island (16.3°N, 166.6°E) at 00 UTC 30 August. The difference between the typhoon track forecasts by the three models is relatively small, but the intensity forecasts vary widely. TL319L40 GSM predicted a rather weak typhoon compared to other models and the best track because of its low horizontal resolution. Higher resolution is needed for better representation of detailed structure of TCs, which is essential for realistic TC intensity forecasts. Meanwhile, TL959L60 GSM and TYM simulated the intensity of the typhoon fairly well as a whole, although a transient feature is seen in the early forecast hours. When generating the typhoon bogus data for the analysis, the typhoon central pressure is increased in most cases for adaptation to the horizontal resolution of the analysis to prevent the initial fields from being distorted by the extreme pressure gap between the inner and outer regions of the TC. This procedure may lead to the transient nature of the time evolution of error in typhoon intensity forecasts by TL959L60 GSM and TYM as seen in Figure 5. Furthermore, the typhoon bogus data is assimilated as observational data produced from the bogus structure in the global analysis, while the bogus structure itself is implanted directly into the first-guess fields in the analysis for TYM. This may also result in a shallower typhoon in the initial fields of TL959L60 GSM. However, it is not clear whether the typhoon represented by TL959L60 GSM and TYM in the early forecast hours is too weak or not. Further investigation is therefore needed on the depth to which a typhoon should be represented in NWP

models with a particular horizontal resolution such as 20 or 24 km. Nevertheless, it seems reasonable to say that TL959L60 GSM predicted the intensity of the typhoon as well as TYM in this case.

3.3 Statistics

Figure 6 shows the mean position error of the typhoon center predicted by TL959L60 GSM, TL319L40 GSM and TYM. The error of TL959L60 GSM is slightly larger than that of TL319L40 GSM. However, the number of cases is so small that the difference is not statistically meaningful. TYM performed the worst of the three models. Using early analysis to make the initial fields and lateral boundary conditions of TYM is not essential because the operational TYM had been outperformed in track forecasts by the operational TL319L40 GSM starting from early analysis (not shown).

The root mean square error (RMSE) and the mean error (ME) of the typhoon central pressure forecasts are shown in Figure 7. The RMSE of TL959L60 GSM is nearly the same as that of TYM, and the difference is insignificant considering the small number of cases. The ME values for TL959L60 GSM and TYM gradually decrease from nearly +12 hPa at the initial time. After the middle forecast hours, the negative ME increases to about -3 hPa in TL959L60 GSM and to about -8 hPa in TYM for 84-hour forecasts. The RMSE of TL319L40 GSM is larger than that of TL959L60 GSM and TYM due to its poor representation of typhoon intensity as shown by the large positive ME.

4. Summary and conclusions

JMA upgraded the resolution of GSM from TL319L40 to TL959L60 in November 2007, when the TYM retired from operational use. Since then, TC track and intensity forecasts have been supported by GSM only, which provides NWP products four times a day for all TCs worldwide. Detailed representation of synoptic and sub-synoptic features such as TC structures in GSM has been

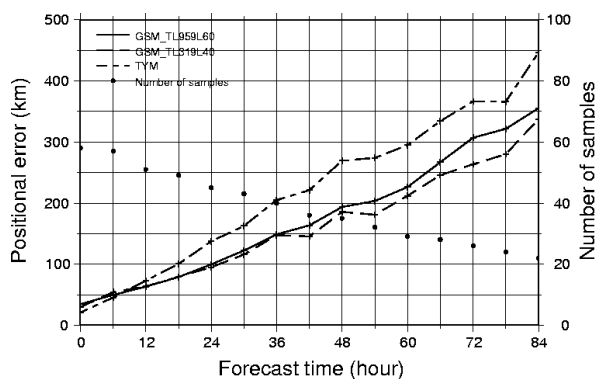


Figure 6 Mean position error of the typhoon center predicted by TL959L60 GSM (solid line), TL319L40 GSM (broken line) and TYM (dot-dash line). The numbers of samples are indicated by the dots.

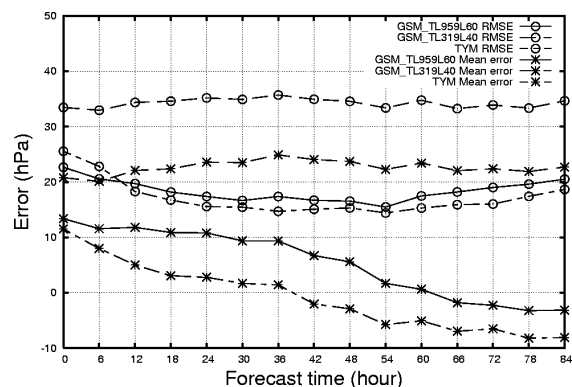


Figure 7 RMSE (circles) and mean error (asterisks) of typhoon central pressure predicted by TL959L60 GSM (solid line), TL319L40 GSM (broken line) and TYM (dot-dash line).

enabled by the enhancement of resolution. In August 2008, a reduced Gaussian grid was implemented in GSM as a new dynamical core that eliminates redundancy by cutting grid points at high latitudes, thus saving on computational resources. Verification of TC forecasts showed that TL959L60 GSM performed better than or as well as TL319L40 GSM and TYM considering the small number of TC cases in the experimental period. TL959L60 GSM also simulated the distribution and intensity of precipitation better than the other two models, including orographic precipitation and heavy rainfall near the center of the TC.

To further improve the accuracy of GSM, JMA plans to upgrade the physical package of the model. The treatment of condensed water in cumulus updraft will be refined to include the detrainment of rainwater and cloud water between the cloud base and the cloud top. The convective downdraft scheme will also be revised to calculate the downdraft ensemble corresponding to the updraft ensemble. Plans are also under way for a mixed-layer ocean model to be coupled with GSM to improve TC intensity forecast. Development of a revised 4D-Var data assimilation system has been started to incorporate the two-time-level semi-Lagrangian advection scheme and the reduced Gaussian grid used in GSM.

Appendix. NWP products

Facsimile charts from NWP are transmitted to local meteorological observatories and weather stations via domestic communication lines, and to National Meteorological Services via GTS. Another set of facsimile charts for users on ships is disseminated by JMH. The contents of the charts are listed in Table A1. The GPV products of NWP are transmitted to JMA's meteorological observatories, weather stations, the Meteorological Satellite Center and the Meteorological Research Institute as well as to the Japan Meteorological Business Support Center (JMBSC). General users in Japan, including private weather service corporations and news media, can obtain GPV products from JMBSC. Specific GPV products are customized and transmitted to relevant governmental organizations. GPV products of GSM are provided to National Meteorological Services through GTS. Two kinds of Internet data service have also been set up to facilitate the use of GPV. One is a data service based on the WMO DDB project (<http://ddb.kishou.go.jp/>), and the other is based on the RSMC DSS. The GPV products of GSM are listed in Table A2.

References

- Iwamura, K. and H. Kitagawa, 2008: An upgrade of the JMA Operational Global NWP Model. CAS/JSC WGNE Res. Act. in Atmos. and Ocea. Modelling, **38**, 6.3-6.4.
- Miyamoto, K., 2006: Introduction of the Reduced Gaussian Grid into the Operational Global NWP Model at JMA. CAS/JSC WGNE Res. Act. in Atmos. and Ocea. Modelling, **36**, 6.9-6.10.
- Nakagawa, M., 2008: Improvement of the Cumulus Parameterization Scheme of the Operational Global NWP Model at JMA. CAS/JSC WGNE Res. Act. in Atmos. and Ocea. Modelling, **38**, 4.9-4.10.

Table A1 List of facsimile charts transmitted through GTS and JMH. Symbols for contents:

Z: geopotential height, ζ : vorticity, T: temperature, D: dewpoint depression, ω : vertical velocity,
W: wind speed by isotach, A: wind arrows, P: sea-level pressure, R: rainfall.

Area	Contents and level	Forecast hours	Initial time	Availability
Far East	500 hPa (Z, ζ)	Analysis	00/12 UTC	GTS
		24, 36	00/12 UTC	GTS/JMH
	500 hPa (T), 700 hPa (D)	24, 36	00/12 UTC	GTS/JMH
	700 hPa (ω), 850 hPa (T, A)	Analysis	00/12 UTC	GTS
		24, 36	00/12 UTC	GTS/JMH
Surface (P, R, A)	24, 36	00/12 UTC	GTS/JMH	
East Asia	300 hPa (Z, T, W, A)	Analysis	00 UTC	GTS
	500 hPa (Z, T, A)	Analysis	00/12 UTC	GTS/JMH
	500 hPa (Z, ζ)	48, 72	00/12 UTC	GTS
	700 hPa (Z, T, D, A)	Analysis	00/12 UTC	GTS
	700 hPa (ω), 850 hPa (T, A)	48, 72	12 UTC	GTS
	850 hPa (Z, T, D, A)	Analysis	00/12 UTC	GTS/JMH
	Surface (P, R)	24	00/12 UTC	GTS
		48, 72	00/12 UTC	JMH
96, 120		12 UTC	JMH	
Asia	500 hPa (Z, ζ)	96, 120, 144, 168, 192	12 UTC	GTS
	850 hPa (T), Surface (P)			
Asia Pacific	200 hPa (Z, T, W), Tropopause (Z)	Analysis	00/12 UTC	GTS
	250 hPa (Z, T, W)	Analysis, 24	00/12 UTC	
	500 hPa (Z, T, W)		00/12 UTC	
Northern Hemisphere	500 hPa (Z, T)	Analysis	12 UTC	GTS
North West Pacific	200 hPa (streamline)	Analysis, 24, 48	00/12 UTC	GTS
	850 hPa (streamline)		00/12 UTC	
	500 hPa (Z, Z anomaly to climatology)			

Xie, S. C. and M. H. Zhang, 2000: Impact of the convective triggering function on single-column model simulations. *J. Geophys. Res.*, **105**, 14983-14996.

Yamaguchi, M. and T. Komori, 2009: Outline of the Typhoon Ensemble Prediction System at the Japan Meteorological Agency. *RSMC Tokyo-Typhoon Center Technical Review*, **11**, 14-24.

Yoshimura, H. and T. Matsumura, 2003: A Semi-Lagrangian Scheme Conservative in the Vertical Direction. *CAS/JSC WGNE Res. Act. in Atmos. and Ocea. Modelling*, **33**, 3.19-3.20.

Table A2 List of GPV products (GRIB) transmitted through GTS, DDB and RSMC DSS.

Symbols for contents: Z: geopotential height, U: eastward wind, V: northward wind, T: temperature, D: dewpoint depression, H: relative humidity, ω : vertical velocity, ζ : vorticity, ψ : stream function, χ : velocity potential, P: sea-level pressure, R: rainfall. Symbols $^{\circ}$, ‡ , † , § , $^{\ulcorner}$ indicate limitations on forecast hours or initial time as shown in the table below.

Destination	GTS	GTS	DDB	DDB
Area and resolution	20°S–60°N, 60°E–160°W 1.25°×1.25°	Whole globe, 2.5°×2.5°	20°S–60°N, 60°E–160°W 1.25°×1.25°	Whole globe, 2.5°×2.5°
Levels and elements	10 hPa: Z,U,V,T 20 hPa: Z,U,V,T 30 hPa: Z,U,V,T 50 hPa: Z,U,V,T 70 hPa: Z,U,V,T 100 hPa: Z,U,V,T 150 hPa: Z,U,V,T 200 hPa: Z [§] ,U [§] ,V [§] ,T [§] , ψ , χ 250 hPa: Z,U,V,T 300 hPa: Z,U,V,T,D 400 hPa: Z,U,V,T,D 500 hPa: Z [§] ,U [§] ,V [§] ,T [§] ,D [§] , ζ 700 hPa: Z [§] ,U [§] ,V [§] ,T [§] ,D [§] , ω 850 hPa: Z [§] ,U [§] ,V [§] ,T [§] ,D [§] , ω , ψ , χ 925 hPa: Z,U,V,T,D, ω 1000 hPa: Z,U,V,T,D Surface: P [¶] ,U [¶] ,V [¶] ,T [¶] ,D [¶] ,R [¶]	10 hPa: Z*,U*,V*,T* 20 hPa: Z*,U*,V*,T* 30 hPa: Z [°] ,U [°] ,V [°] ,T [°] 50 hPa: Z [°] ,U [°] ,V [°] ,T [°] 70 hPa: Z [°] ,U [°] ,V [°] ,T [°] 100 hPa: Z [°] ,U [°] ,V [°] ,T [°] 150 hPa: Z*,U*,V*,T* 200 hPa: Z,U,V,T 250 hPa: Z [°] ,U [°] ,V [°] ,T [°] 300 hPa: Z,U,V,T,D* [‡] 400 hPa: Z*,U*,V*,T*,D* [‡] 500 hPa: Z,U,V,T,D* [‡] 700 hPa: Z,U,V,T,D 850 hPa: Z,U,V,T,D 1000 hPa: Z,U*,V*,T*,D* [‡] Surface: P,U,V,T,D* [‡] ,R [†]	100 hPa: Z,U,V,T 150 hPa: Z,U,V,T 200 hPa: Z,U,V,T, ψ , χ 250 hPa: Z,U,V,T 300 hPa: Z,U,V,T,D 400 hPa: Z,U,V,T,D 500 hPa: Z,U,V,T,D, ζ 700 hPa: Z,U,V,T,D, ω 850 hPa: Z,U,V,T,D, ω , ψ , χ 925 hPa: Z,U,V,T,D, ω 1000 hPa: Z,U,V,T,D Surface: P,U,V,T,D,R	100 hPa: Z,U,V,T 200 hPa: Z,U,V,T 250 hPa: Z,U,V,T 300 hPa: Z,U,V,T 500 hPa: Z,U,V,T 700 hPa: Z,U,V,T,D 850 hPa: Z,U,V,T,D Surface: P,U,V,T,D,R [†]
Forecast hours	0–84 every 6 hours [§] additional 96–192 every 24 hours for 12 UTC [¶] 0–192 every 6 hours	0–72 every 24 hours and 96–192 every 24 hours for 12 UTC [°] 0–120 for 12 UTC [‡] Except analysis [*] Analysis only	0–72 every 6 hours	0–72 every 24 hours [†] Except analysis
Initial times	00 UTC, 06 UTC, 18 UTC and 12 UTC	00 UTC and 12 UTC [‡] 00 UTC only	00 UTC and 12 UTC	12 UTC

Table A2 (cont.)

Destination	RSMC DSS	RSMC DSS	RSMC DSS	RSMC DSS
Area and resolution	Whole globe, 1.25°×1.25°	20°S–60°N, 60°E–160°W 1.25°×1.25°	Whole globe, 2.5°×2.5°	20°S–60°N, 80°S–160°W 2.5°×2.5°
Levels and elements	10 hPa: Z,U,V,T 20 hPa: Z,U,V,T 30 hPa: Z,U,V,T 50 hPa: Z,U,V,T 70 hPa: Z,U,V,T 100 hPa: Z,U,V,T 150 hPa: Z,U,V,T 200 hPa: Z,U,V,T,ψ,χ 250 hPa: Z,U,V,T 300 hPa: Z,U,V,T,H,ω 400 hPa: Z,U,V,T,H,ω 500 hPa: Z,U,V,T,H,ω,ζ 600 hPa: Z,U,V,T,H,ω 700 hPa: Z,U,V,T,H,ω 850 hPa: Z,U,V,T,H,ω,ψ,χ 925 hPa: Z,U,V,T,H,ω 1000 hPa: Z,U,V,T,H,ω Surface: P,U,V,T,H,R†	10 hPa: Z,U,V,T 20 hPa: Z,U,V,T 30 hPa: Z,U,V,T 50 hPa: Z,U,V,T 70 hPa: Z,U,V,T 100 hPa: Z,U,V,T 150 hPa: Z,U,V,T 200 hPa: Z [§] ,U [§] ,V [§] ,T [§] ,ψ,χ 250 hPa: Z,U,V,T 300 hPa: Z,U,V,T,D 400 hPa: Z,U,V,T,D 500 hPa: Z [§] ,U [§] ,V [§] ,T [§] ,D [§] ,ζ 700 hPa: Z [§] ,U [§] ,V [§] ,T [§] ,D [§] ,ω 850 hPa: Z [§] ,U [§] ,V [§] ,T [§] ,D [§] ,ω, ψ,χ 925 hPa: Z,U,V,T,D,ω 1000 hPa: Z,U,V,T,D Surface: P [¶] ,U [¶] ,V [¶] ,T [¶] ,D [¶] ,R [¶]	10 hPa: Z*,U*,V*,T* 20 hPa: Z*,U*,V*,T* 30 hPa: Z*,U*,V*,T* 50 hPa: Z*,U*,V*,T* 70 hPa: Z*,U*,V*,T* 100 hPa: Z°,U°,V°,T° 150 hPa: Z*,U*,V*,T* 200 hPa: Z,U,V,T 250 hPa: Z°,U°,V°,T° 300 hPa: Z,U,V,T,D*‡ 400 hPa: Z*,U*,V*,T*,D*‡ 500 hPa: Z,U,V,T,D*‡ 700 hPa: Z,U,V,T,D 850 hPa: Z,U,V,T,D 1000 hPa: Z*,U*,V*,T*,D*‡ Surface: P,U,V,T,D*‡,R†	100 hPa: Z,U,V,T 150 hPa: Z,U,V,T 200 hPa: Z,U,V,T 250 hPa: Z,U,V,T 300 hPa: Z,U,V,T 500 hPa: Z,U,V,T,D,ζ 700 hPa: Z,U,V,T,D,ω 850 hPa: Z,U,V,T,D,ω Surface: P,U,V,T,D,R
Forecast hours	0–84 every 6 hours and 96–192 every 12 hours † Except analysis	0–84 every 6 hours § additional 96–192 every 24 hours for 12 UTC ¶ 0–192 every 6 hours	0–72 every 24 hours and 96–192 every 24 hours for 12 UTC ° 0–120 for 12 UTC † Except analysis * Analysis only	0–36 every 6 hours, 48, 60, and 72 hours
Initial times	00 UTC, 06 UTC, 18 UTC and 12 UTC	00 UTC, 06 UTC, 18 UTC and 12 UTC	00 UTC and 12 UTC ‡ 00UTC only	00 UTC and 12 UTC